論文

수지이동 성형공정에서 섬유직조망내의 수지유동에 관한 연구

김성우* · 이종훈** · 이미혜*** · 남재도**** · 이기준**

A Study on the Resin Flow through Fibrous Preforms in the Resin Transfer Molding Process

Seong Woo Kim*, Chong Hoon Lee**, Mi Hye Lee***, Jae-Do Nam**** and Ki-Jun Lee**

초 록

고분자 복합재료 제조공정인 수지이동성형(RTM) 공정은 최근 들어서 고성능 재료를 필요로 하는 항공산업분야에서 관심의 대상이 되고 있다. 본 연구에서는 유한요소/관할부피 기법을 도입한 수치모사를 통해서 수지이동 성형공정에서의 금형충전단계를 해석하였다. 섬유직조망의 투과계수를 정량적으로 측정하고, 또한 수치모사에 이용된 프로그램을 검증하기 위하여 유동가시화 실험을 수행하였다. 실험에 사용된 강화섬유와 수지물질로는 여러 가지 형태의 섬유직조망과 실리콘 기름을 선택하였다. 수치모사와 유동가시화 실험을 병행함으로써 섬유직조망의 구조, 금형의 구조, 금형삽입체가 금형충전단계에서의 수지 유동선단의 형태에 미치는 영향을 살펴보았다. 모델링에 의해 예측된 유동선단은 유동가시화 실험을 통해 관찰된 결과와 잘 일치한 것으로 나타났으나, 금형내 불균일한 섬유부피분율로 인해 섬유직조망의 투과계수가 전 영역에서 일정한 값을 가지지 못하기 때문에 약간의 차이를 보여주었다. 원형의 구조물이 금형내에 삽입되어 있는 경우, 웰드라인의 위치를 예측된 유동선단으로부터 정성적으로 추정할 수 있었다.

ABSTRACT

Resin transfer molding(RTM) as a composite manufacturing process is currently of great interest in the aerospace industry requiring high performance composite parts. In this study, an analysis of mold filling in the RTM process was carried out by numerical simulation using finite elememt/control volume technique. Experimental work for the visualization of resin flow through fibrous preform was also conducted in order to quantitatively measure the permeabilities of the fiber mats and to evaluate the validity of the developed numerical code. The different types of fiber mats and silicon oils were selected as reinforcements and resin materials, respectively. The effects of fibrous preform structure, mold geometry, and preplaced insert on the flow front patterns during mold filling were examined by integrating the model predictions and experimental results. The flow fronts predicted by numerical simulation were in good agreement with those observed experimentally. However, according to the regions of the mold, some deviations between predicted and observed flow fronts could be found because of non-uniform fiber volume fraction. Weldline locations for the resin flow through round insert preplaced in the mold could be qualitatively deduced based on predicted flow fronts.

* 경기대학교 화학공학과
** 서울대학교 응용화학부
*** 부산/울산 지방중소기업청
**** 성균관대학교 고분자 공학과

1. INTRODUCTION

Resin transfer molding(RTM) as a composite manufacturing process is currently of great interest in such a high-performance environment as aerospace due primarily to its design flexibility and economics. RTM is a versatile and efficient process for producing fiber-reinforced polymer composite structures from small articles of simple shape to large articles with complex shape. In addition, RTM has processing advantages over prepreg/autoclave technique providing fast cycle time, low capital investment, no bagging labour, and no storage problem of B-staged prepregs.

Resin flow through fibrous preform during mold filling process is largely dependent upon the structure of the network. Hence, an identification of permeability for the fibrous material is significant in the design and processing of resin transfer molding.

In general, permeability of a fibrous network is governed by the structural factors such as weave type, weave balance, fiber packing density, and fiber orientation[1]. Visualization study of resin flow through fibrous preform is essential in order to measure intrinsic parameters of the fiber mats and also to examine specific problems such as void formation and fiber washout during mold filling process.

Several methods have been reported for measuring the permeability of the fiber mats in both the transverse and in-plane flow directions during consolidation process.

Gutowski et al.[2] performed experiments on special prepregs made of constant viscosity oils and aligned graphite fibers to investigate the fiber deformation behavior and permeability. They have confirmed that the fiber network acts like a non-linear elastic porous medium, and that the permeability of fiber bundle is strongly dependent on both anisotropy and fiber volume fraction. Analytical and experimental studies in which free surface effects were considered have been reported by Williams et al.[3] and Adams et al.[4]. Ahn et al.[5] measured the unsteady state permeability and the capillary pressure due to the resin matrix surface tension simultaneously in a composite impregnation process. They also claimed that the thickness and permeability of both the interfacial and fabric layers should be considered at high porosities in calculating permeability.

Recently, Dave[6] derived the models for resin flow during composite processing in terms of the Darcy' s law applying the unified approach. He showed that the resin flow models for autoclave processing, pultrusion, and resin transfer molding are specific cases of a generalized theory. Coulter and G ceri[7] have reported on the numerical and experimental investigations of resin impregnation during RTM process in irregularly shaped two-dimensional domains. They used boundary-fitted coordinates system with numerical grid generation to simulate the in-plane flow through a fibrous medium. Bruschke and Advani[8] presented a numerical simulation based on the finite element/control volume method to predict the movement of a free surface flow front through a fiber network in a thin shell mold geometry of arbitrary shape. Experiments were carried out in a flat rectangular mold using a Newtonian fluid in order to verify the numerical model. Chan and Hwang[9] have developed a model for simulating isothermal mold filling based on Galerkin finite element method during RTM of polymeric composites. They took into account the anisotropic characteristic of the fibrous network and viscosity variations of the resin due to the chemical reaction. Recently, Choi et al.[10] developed computational program for numerical modeling of mold filling in the RTM process. In this numerical simulation, the finite element method and the mesh generation technique was used to handle the changing flow domain shape during mold filling.

In the present study, numerical simulation was carried out based on finite element /control volume method to predict the flow pattern for mold

filling of fluids through fibrous preform and to investigate the relationship between processing variables, material properties, and flow variables from numerical results. Experimental work for the visualization of resin flow through fibrous preform was also performed in order to measure permeability parameters of fiber mats to be utilized in numerical modeling and to provide some data for comparison with results predicted by numerical code developed. The different types of fiber mats such as bleeder, random glass fiber mat, a bidirectional glass fiber mat, and plain-weave carbon fiber mat, are selected as reinforcements in this work.

2. THEORETICAL BACKGROUND

2.1. Anisotropic Permeabilities

In order to determine anisotropic permeabilities of the unsaturated fibrous preform during RTM process, several assumptions were made to simplify In this study: (1) the preplaced fiber mats in the mold cavity are assumed rigid and no deformation occurs during mold filling; (2) capillary and inertia effects are neglected due to slow resin flow; (3) surface tension is neglected compared to the dominant viscous force; (4) when the filling time is sufficiently long, the transient flow is reasonably approximated by a pseudo-steady state assumption. Then, the momentum equation for flow through porous media from Darcy's law can be written as

$$\mathbf{v} = -\frac{\mathbf{K}}{\mu} \cdot \nabla P \tag{1}$$

where $\mathbf{v}$ is velocity vector, μ is fluid viscosity, P is the pressure, and $\mathbf{K}$ is the permeability tensor. For an incompressible fluid, the continuity equation is as follows.

$$\nabla \cdot \mathbf{v} = 0 \tag{2}$$

If the coordinate axes are so chosen that their directions match the principal directions of the fiber mats, the cross terms in the permeability tensor become zero and non-zero terms remain in the diagonal entries of the tensor. Substituting eq.(1) into eq.(2) and aligning the axes to the principal directions of the fiber mat,

$$\nabla \cdot \left[\frac{1}{\mu} \mathbf{K} \cdot \nabla P \right] = 0 \tag{3}$$

In RTM simulation, the dimension of thickness is much smaller than the dimensions in the planar direction, and the mold filling in a thin cavity can be modeled as two-dimensional. When the anisotropic permeabilities are assumed constant with respect to position, eq.(3) in the $x-y$ coordinate system can be expressed as

$$\frac{\partial^2 P}{\partial x^2} + \delta \frac{\partial^2 P}{\partial y^2} = 0 \tag{4}$$

where the ratio of the two in-plane permeabilities is defined as $\delta = K_2/K_1$, and K_1 and K_2 are permeabilities in the x and y principal directions, respectively.

Solving the governing equations for the moving front, the moving boundary can be described by exact and iterative equations for both isotropic and anisotropic porous media, respectively[1,4, 11,12]. For an isotropic porous medium(δ=1), the fluid front is macroscopically circular and the pressure varies only radially. When R_o and R_f are the radius of circular boundary of fluid at t=0 and t=t, respectively, the dimensionless radial extent, $\rho_d = R_f/R_o$, of an isotropic porous medium is obtained as a function of time:

$$G(\rho_d) = \rho_d^2(2 \ln \rho_d - 1) + 1 = 4\Phi \tag{5}$$

where $\frac{4K \triangle P}{\phi \mu R_o^2} t$ is dimensionless time, and ϕ is porosity.

For an anisotropic fiber network, the solution of the differential equation exhibits an ellipse-like moving boundaries expressed as

$$F(\xi_f, \eta) = (\xi_f - \xi_0)\left[\frac{\sinh(2\xi_f)}{4} + \frac{\xi_f}{2}\right] - \frac{\cos^2\eta\,(\xi_f-\xi_0)^2}{2} + \frac{\cosh(2\xi_0)-\cosh(2\xi_f)}{8} + \frac{\xi_0^2-\xi_f^2}{4} = \left(\frac{\delta}{1-\delta}\right)\Phi \quad (6)$$

where

$$\xi_o = \ln\left[\frac{1+\delta^{0.5}}{(1-\delta)^{0.5}}\right] \quad (7)$$

$$\xi_{f1} = \sinh^{-1}\left[\frac{R_{f_1}}{R_o}\,(1/\delta-1)^{-0.5}\right] \quad (8)$$

$$\xi_{f2} = \cosh^{-1}\left[\frac{R_{f_2}}{R_o}\,(1-\delta)^{-0.5}\right] \quad (9)$$

ξ_0 and ξ_f are the elliptical equivalent of the inlet boundary and resin front, respectively, ξ_{f1} and ξ_{f2} represent the principal direction 1 and 2, respectively η is the elliptical equivalent of the in-plane angle, and the dimensionless time Φ is based on K_1. The anisotropic data is analyzed iteratively with respect to δ, providing the best fit line in the $F(\xi,\eta)$ vs. time relation[4].

2.2. Numerical Simulation

In the finite element/control volume method for a two-dimensional flow, the calculation domain can be divided into three noded triangular elements. Then, the centroids of the elements are joined to the midpoints of the three corresponding sides, creating polygonal control volumes surrounding each vertex node in the calculation domain. The pressure field expressed by eq.(4) within an element(l) can be approximated by three nodal pressures, $P_k^{(l)}$, k =1, 2, 3, and three interpolation functions, $\Psi_k^{(l)}(x, y)$:

$$P^{(l)}(x, y) = \sum_{k=1}^{3} \Psi_k^{(l)}(x, y) P_k^{(l)} \quad (10)$$

The shape function has the form

$$\Psi_k^{(l)}(x, y) = a_{1k}^{(l)} + a_{2k}^{(l)} x + a_{3k}^{(l)} y \quad (11)$$

where the a_{ik} coefficient are chosen to make $\Psi_k^{(l)}(x, y)$ equal to unity at node k and zero at the other two nodes.

For a two-dimensional case, the net flow into a control volume in element l can be expressed by a line integral of the velocity along its boundary, namely,

$$q = 2b \int_c \mathbf{u} \cdot \mathbf{n}\, ds = 2b \int_c u dy - v\, dx \quad (12)$$

where $\mathbf{n}$ is a unit normal vector to the boundary, u and v are average velocity in element l in the x and y direction, respectively, and b is the half-thickness in the z direction.

Substituting eqs. (1), (7), and (8) into (9), the net flow $q_i^{(l)}$ that enters the control volume of nodal point N from an element (l) can be expressed as

$$q_i^{(l)} = \frac{b}{\mu} \sum_{k=1}^{3} D_{ik}^{(l)} P_N \quad (13)$$

i = 1, 2, or 3 (nodal points in an element)

where D_{ik} is a 3×3 symmetric matrix with the entries expressed by the shape function coefficients as

$$\begin{aligned}
D_{11}^{(l)} &= -a_{21}^{(l)} a_{21}^{(l)} - a_{31}^{(l)} a_{31}^{(l)} \delta \\
D_{22}^{(l)} &= -a_{22}^{(l)} a_{22}^{(l)} - a_{32}^{(l)} a_{32}^{(l)} \delta \\
D_{33}^{(l)} &= -a_{23}^{(l)} a_{23}^{(l)} - a_{33}^{(l)} a_{33}^{(l)} \delta \\
D_{12}^{(l)} &= D_{21}^{(l)} = -a_{21}^{(l)} a_{22}^{(l)} - a_{31}^{(l)} a_{32}^{(l)} \delta \\
D_{13}^{(l)} &= D_{31}^{(l)} = -a_{23}^{(l)} a_{21}^{(l)} - a_{33}^{(l)} a_{31}^{(l)} \delta \\
D_{23}^{(l)} &= D_{32}^{(l)} = -a_{22}^{(l)} a_{23}^{(l)} - a_{32}^{(l)} a_{33}^{(l)} \delta
\end{aligned} \quad (14)$$

From the mass conservation, the sum of all incoming net flow to the control volume around N should be zero, viz:

$$\sum_{l} q_i^{(l)} = \frac{b}{\mu} \sum_{l} \sum_{k}^{3} D_{ik}^{(l)} P_N = 0 \qquad (15)$$

where (l) and N' denotes all the triangular elements and nodal points containing node N. The above equation can be applied to all the nodes in the flow field, which consequently results in a set linear algebraic equations. It should also be noted that the Galerkin formulation leads to the same descretization equation as the control volume method in the diffusion-type problem[13]. As boundary conditions of the differential equation, the pressure gradient normal to the solid wall was set to zero, and a constant pressure was assumed at the flow front.

Since the mold filling is a transient process and the flow front is advancing with time, the pressure equations are valid only in the fluid region. Using the flow analysis network method, in this study, each node was classified with specific value f: entrance node(f=1), interior node(f=1), flow front node(0<f<1), empty node(f=0)[14,15]. The polygonal control volumes had the desirable property that they span the calculation domain completely without overlapping. In the calculation domain, the parameter f as a fill factor represent the status of each control volume, i.e., the volumetric fraction of the fluid inside the control volume at a given time.

After solving the system equation for pressure field, the net flow front was estimated by the velocity vector in the flow front at each time step. According to the quasi-steady state approximation, the time increment was so chosen that one control volume was completely filled in each time step.

It has been found that equilateral triangular elements give the least oscillation in the shape of the advancing front[13]. Therefore a uniform distribution of equilateral triangular elements is recommended for better predictions of the flow front. The typical mesh configuration employed in this study is shown in Fig. 1. The mesh configuration was made by using the automesh program of the C-FLOW software package. As shown in the figure, the calculation domain, composing of 1596 elements and 869 nodes, could be nearly be divided into equilateral triangular elements.

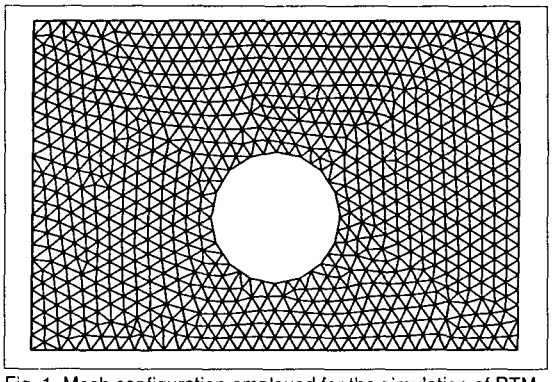

Fig. 1. Mesh configuration employed for the simulation of RTM process using finite element/control volume method.

3. EXPERIMENTAL

The experimental work was performed for the flow visualization and measurement of permeability using the mold filling apparatus shown in Fig. 2. The top plate of the mold is made of clear acrylic plate so that progress of the resin flow

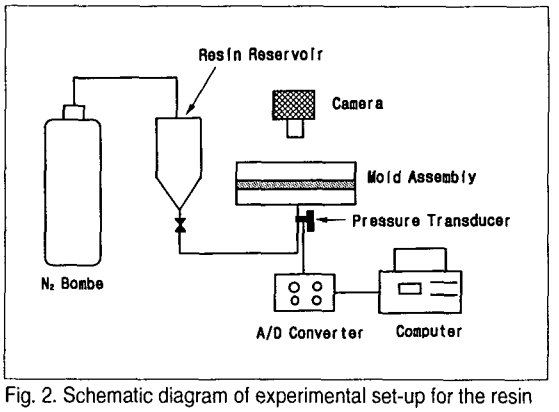

Fig. 2. Schematic diagram of experimental set-up for the resin flow visualization.

front can be observed during filling process. The fiber mats were surrounded by a sealant tape for preventing movement of the fibrous preform as well as sealing around the edge of the mold. And then, the fiber mats were sandwiched between a 2.0 cm thick aluminum base plate and a 2.0 cm thick acrylic top plate. The mold gap height could be adjusted by inserting spacer plate with different thickness.

Two specific injection conditions were investigated for resin flow visualization experiment: maintaining a constant injection pressure or a constant inlet flow rate.

The resin pressurized with N_2 gas in a cylinder resin reservoir was injected throughpolyurethane tube at a constant injection pressure. For the case of a constant inlet flow rate of resin, the liquid in the reservoir was forced to flow by a piston connected to the crosshead of a universal testing machine(Instron), which was programmed to move at a constant rate. The mold inlet pressure as a function of time during mold filling was measured by mounting a pressure transducer(VPRF, Valcom Inc.) in the base plate near the inlet.

The fluids used in these experiment were silicon oils exhibiting Newtonian behavior over the shear rate tested, which were supplied by Shin-Etsu Chem. Co. Ltd. Various types of fiber mats, such as bleeder for absorbing excess resin during composite manufacturing, random glass fiber mat, carbon fiber mat of plain weave pattern, and a bidirectional glass mat, were selected as reinforcements in this study.

The resin was mixed with dyes manufactured by BASF so that the progression of the resin front could clearly be observed. The pictures of the resin front were taken with a camera at an arbitrary time interval and inlet gauge pressure was recorded until filling process was completed. Experiments were run under isothermal room temperature conditions.

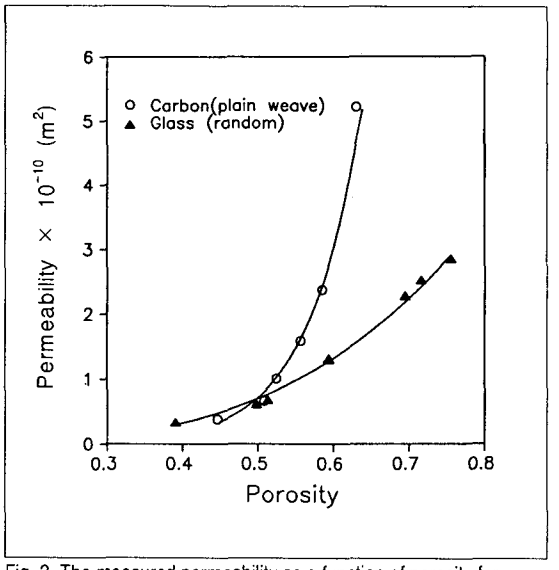

Fig. 3. The measured permeability as a function of porosity for isotropic woven carbon fiber mat and random glass fiber mat.

4. RESULTS AND DISCUSSION

The in-plane permeabilities as a function of porosity for the plain weave carbon fiber and random glass mats were measured as shown in Fig. 3. These two fabric systems were found to exhibit an

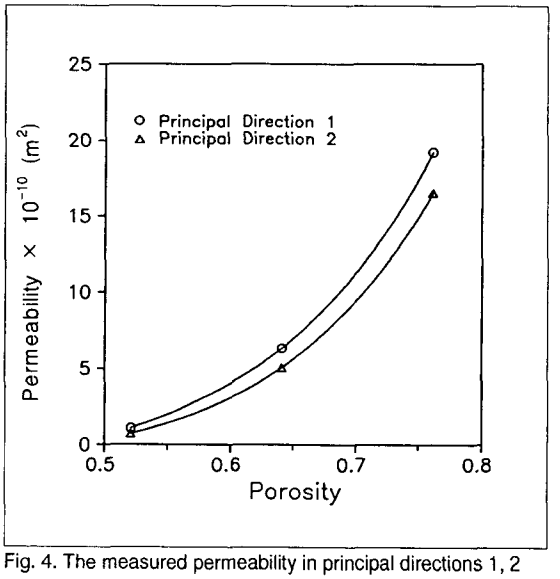

Fig. 4. The measured permeability in principal directions 1, 2 for the anisotropic bidirectional glass fiber mat.

isotropic characteristic in the fluid flow through the porous media. The permeability of carbon fiber mat is higher than that of random glass fiber mat in the range of porosity from 0.5 to 0.76. This may be attributed to the rough surfaces due to the weaving patterns of the carbon fiber. If porosity is low, the fabric layers make an intimate contact so that the interface between fabric plies can be neglected. As the porosity increases, the fabric preform becomes heterogeneous, such that the interlayer porosity is higher than the intralayer porosity.

The measured permeabilities for different porosities of the bidirectional glass fiber mat are shown in Fig. 4. This fiber mat exhibited anisotropic characteristic in the two principal directions 1, 2 designated by the wrap and fill directions of the yarn.

As the porosity of bidirectional glass fiber mat decreases, the degree of anisotropy becomes higher (i.e. K_2/K_1 is small) even though the difference between two principal permeabilities is small. The reason for this behavior is that higher clamping force required to maintain small porosity of the fibrous preform preplaced inside mold can induce the deformation of fiber network, which may result in higher degree of anisotropy.

Using the measured permeabilities of the fibrous preforms, the predicted flow fronts by numerical simulation were compared with the observed flow fronts through visualization experiments conducted under various conditions. The various conditions used in flow visualization experiments are summarized in Table 1.

The comparisons of the progressions of the flow front predicted by numerical simulations based on finite element/control volume method and observed experimentally(Exp.1) are shown in Fig. 5. As can be seen, the predicted and observed flow fronts during mold filling through preplaced bleeder agree well in the air vent region. However, the reason for discrepancy in the air vent free region is that a zero pressure value along the flow front is assumed for the numerical simulation. The fiber mats which exist along the front at any given time during the process may actually exert some force on the front due to the air compression.

Macroscopically, the summation of these many small force components which exist at distinct points along the front may be viewed as a net non-zero pressure exerted on the entire front.

Fig. 6 represents the comparisons of the resin fronts predicted by numerical simulation and observed flow fronts(Exp.2) for the same mold geometry system when resin impregnates the random glass fiber mat at a constant inlet flow rate of 0.08 cm^3/sec. Since the gate is located at the center of the mold, the fluid comes in at the center and flows out radially. The speed of piston, which was connected to the crosshead of a constant speed Instron testing machine, was selected as 0.42 mm/min in the resin reservoir to provide constant inlet flow rate of 0.08 cm^3/sec. In order to remove the influence of air compression, four air

Table 1. The various conditions used in flow visualization experiments.

	Exp.1	Exp2	Exp3	Exp4	Exp5
Mold Dimension(cm)	20×20	20×20	20×20	15×10	15×10
Gate Position	center	center	center	corner	corner
Gap Height(mm)	4.0	2.5	2.0	1.5	1.5
Insert	-	-	round insert	-	round insert
Resin Viscosity(Pa · s)	7.6	2.7	2.7	2.7	2.7
No. of Plies	2	5	5	5	5
Porosity	0.936	0.766	0.707	0.609	0.609
Permeability(m^2)	2.8×10^{-9}	2.85×10^{-10}	2.27×10^{-10}	1.30×10^{-10}	1.30×10^{-10}

vents were positioned at four corners along the perimeter of the mold. The experimental and predicted flow front correspond well. However, the flow front observed in the experiment moves faster than that predicted by numerical simulation in the upper area of the mold. This is attributed to the non-uniform fiber volume fraction of the random glass fiber mat which may result in lower permeability in this area. Therefore, in order to overcome this problem, higher permeability values should be assigned to the nodes of each element in this numerical region for modeling of resin flow through dry fiber mats.

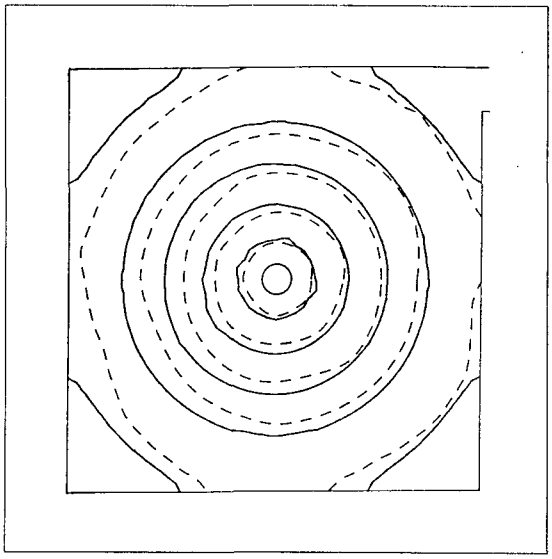

Fig. 5. The experimental and predicted flow fronts during moldfilling under constant inlet pressure of 72.4 kPa.(t = 5, 35, 110, 240, 550 sec)
——— simulation, - - - - - - - - experiment

In other words, according to the region of the fiber mat, different permeability values should be used for the numerical simulation to model resin flow phenomena more accurately.

Fig. 7 shows the comparison of the resin fronts predicted and observed(Exp.3) during mold filling with preplaced round insert. For this case, the resin impregnates the random glass fiber mats in the mold under the constant inlet pressure of 53.8 kPa. The boundary conditions imposed at the insert are the same as those at the mold walls. The predicted flow fronts are in good agreement with

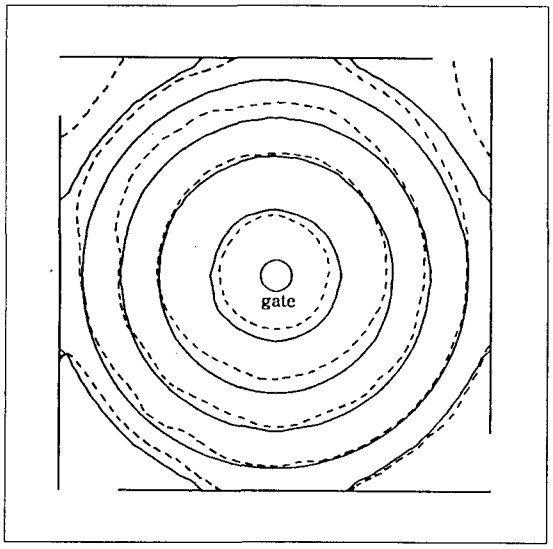

Fig. 6. Comparison of the predicted and observed flow fronts when resin impregnates the random glass fiber mat at a constant inlet flow rate of 0.08 cm3/sec.(t = 70, 230, 400, 620, 790 sec)
——— simulation, - - - - - - - - experiment

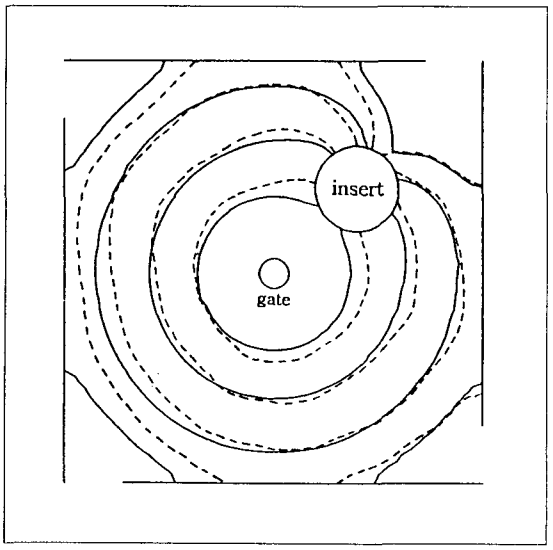

Fig. 7. Comparison of the observed and predicted flow fronts for the mold geometry with round insert when inletpressure is 53.8 kPa. (t = 80, 270, 610, 870 sec)
——— simulation, - - - - - - - - experiment

those experimentally until the front reaches the mold wall. The fiber mat near the wall is compressed due to the sealant tape surrounded around the side wall of the mold, which may result in higher volume fraction of the fiber in this area. Therefore, higher flow resistance through the fiber mat with lower permeability values near the wall can actually slow the advancement of the flow front.

Since the thermoset resin matrix can be hardened due to cure process during mold filling of the actual RTM process, an investigation on the weldline formation, which may influence the mechanical property of the cured composite material, is significant in manufacturing composite materials. It is noted that although the simulation can not predict the weldline location explicitly, one can usually deduce its position based on where the two flow fronts first meet together and on the flow front shapes at succeeding time steps. In the present case, the predictions are seen to be very compatible with the experimental weldline position.

The prediction of the resin front for the different mold geometry system with corner gate, of which length is 2.7 cm, is compared with observed flow front(Exp.4) in Fig. 8. The resin is injected into the mold with preplaced random glass fiber mat under the constant inlet pressure of 110.3 kPa. In this case, higher inlet pressure is required to inject the resin through fiber mat, because for the corner gate, the flow path inside the mold is much longer than for the centered hole gate. The predicted flow front follows the same trend with the experimental result. However, the deviation between predicted flow front and observed result becomes larger with time.

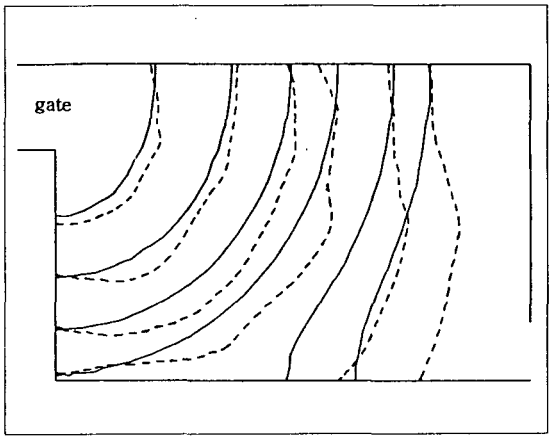

Fig. 8. Comparison of the progression of the predicted and observedflow fronts for the mold geometry with corner gate under constant inlet pressure of 110.3 kPa.(t = 150, 550, 1100, 1700, 2600, 3200 sec)
——— simulation, -------- experiment

This discrepancy may be caused by one of two factors. The first of these is the flow channelling phenomena between the reinforcement and surface of the mold. The second factor is the local permeability variations resulting from the non-uniform fiber volume fraction throughout fibrous preform.

The predicted pressure distribution for this case is depicted in Fig. 9. As seen in the figure, The pressure distribution shows a large pressure gradient near the mold inlet, and gradually decreases as distance from the inlet increases. The highest pressure region is distributed near the corner of the mold, where gate is located.

High pressure near the mold gate implies a need of higher clamping force or a potential leakage problem during mold filling process. Accordingly, the mold system with centered hole gate would be the better design for thin parts with large surface area.

Fig. 10 represents the comparison of the predicted and observed flow fronts(Exp.5) for the mold filling with round insert when inlet pressure is constant as 110.0 kPa.

From the figure, it can be seen that numerical results agree well with the flow front observed experimentally.

5. CONCLUSIONS

In the resin transfer molding(RTM) as composite manufacturing process, resin flow phenomena

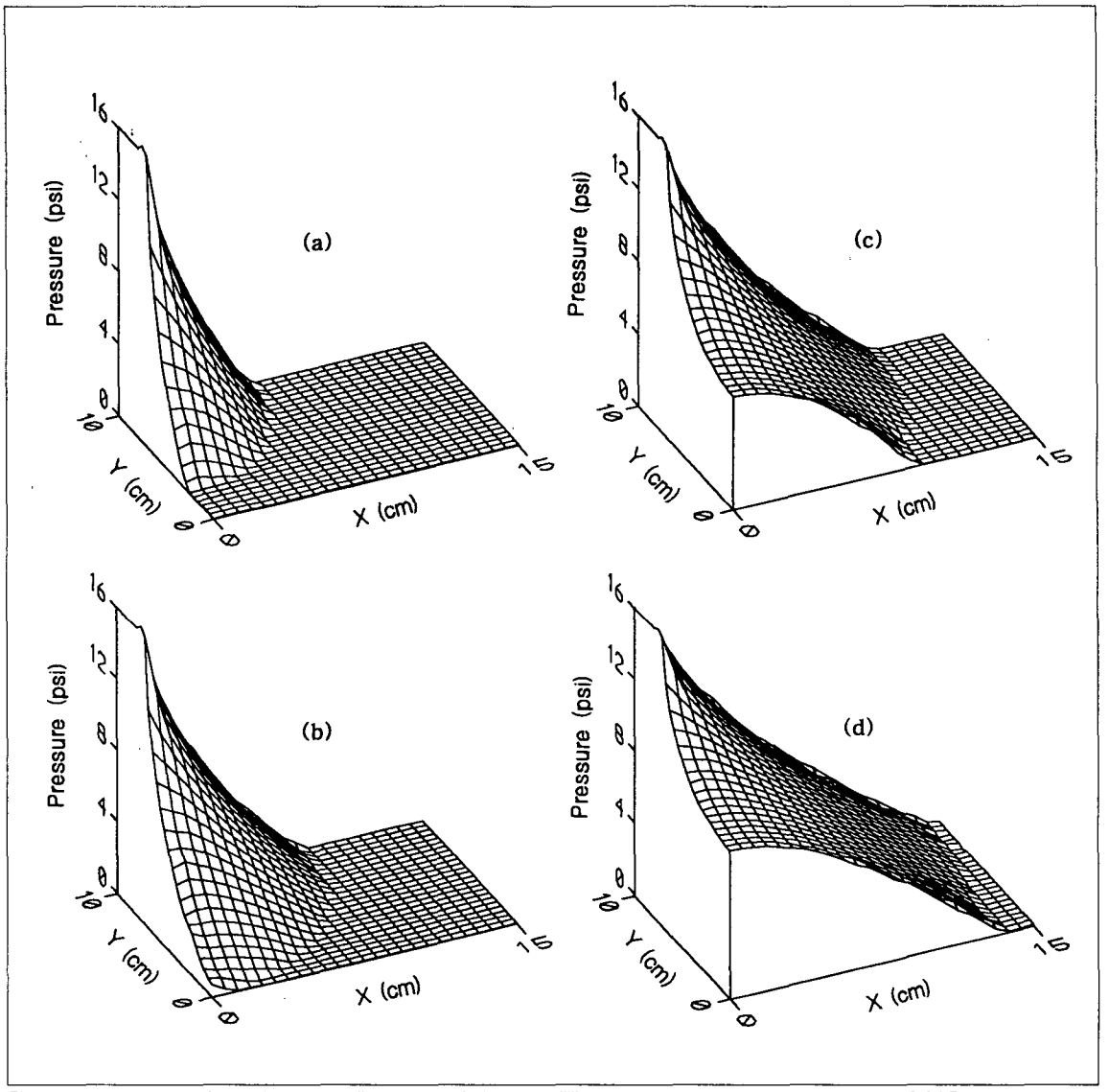

Fig. 9. Pressure distribution at the intermediate stages during mold filling when inlet pressure is constant as 110.3 kPa.
(a) 738 sec (b) 1759 sec (c) 2998 sec (d) 4649 sec ——— simulation, -------- experiment

through fibrous preforms were analyzed by numerical modeling. The developed numerical code based on finite element/control volume method was validated through comparisons between predicted and observed resin flow fronts during mold filling. Experimental work for the resin flow visualization during impregnation process was also performed to measure the permeabilities of the fiber mats to be used in the numerical simulation and to examine specific problems involved during impregnation process.

The flow fronts predicted by numerical simulation using finite element/control volume scheme were in good agreement with those observed

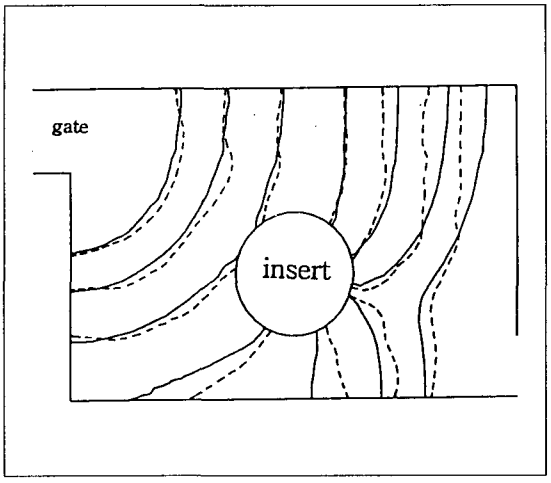

Fig. 10. Comparison of the observed and predicted flow fronts for the corner gate mold geometry with round insert using constant inlet pressure of 111.0 kPa. (t = 170, 370, 750, 1300, 1800, 2400, 3000 sec)
——— simulation, -------- experiment

experimentally during impregnation process for the various mold geometry systems. However, some deviations between predicted and observed flow fronts were found in the some region of the mold, which may be attributed to the non-uniform fiber volume fraction resulting in different permeabilities. Weldline location for the mold geometry with preplaced round insert could be qualitatively deduced based on predicted resin flow fronts. The present study carried out by both modeling and experiments is expected to provide valuable information for the mold design and processing in the RTM process.

REFERENCES

1. Adams, K. L. and Rebenfeld, L., "In-Plane Flow of Fluids in Fabrics : Structure/Flow Characterization", Textile Res. J., Vol.57, 1987, p.647.

2. Gutowski, T. G., Cai, Z., Bauer, S., Boucher, D., Kingery, J., and Winwman, S., "Consolidation Experiments for Laminate Composites", J. Compos. Mater., Vol.21, 1987, p.650.

3. Williams, J. C., Morris, C. E. M., and Ennis, B. C., "Liquid Flow through Aligned Fiber Beds", Polym. Eng. Sci., Vol.14, 1974, p.413.

4. Adams, K. L., Russel, W. B., and Rebenfeld, L., "Radial Penetration of a Viscous Liquid into a Planar Anisotropic Porous Medium", Int. J. Multiphase Flow, Vol.14, 1988, p.203.

5. Ahn, K. J. and Seferis, J. C., "Simultaneous Measurements of Permeability and Capillary Pressure of Thermosetting Matrices in Woven Fabric Reinforcements", Polym. Compos., Vol.12, 1991, p.146.

6. Dave, R., "A Unified Approach to Modeling Resin Flow during Composite Processing", J. Compos. Mater., Vol.24, 1990, p.22.

7. Coulter, J. P., Smith, B. F., and G ceri, S. I., "Experimental and Numerical Analysis of Resin Impregnation During the Manufacturing of Composite Materials",Proceedings. 2nd Technical Conference American Society for Composites, 1987, p.209.

8. Bruschke, M. V. and Advani, S. G., "A finite Element/Control Volume Approach to Mold Filling in Anisotropic Porous Media", Polym. compos., Vol.11, 1990, p.398.

9. Chan, A. W. and Hwang, S. T., "Modeling of the Impregnation Process During Resin Transfer Molding", Polym. Eng. Sci., Vol.31, 1991, p.1149

10. Choi, M. A., Lee, M. H., Lee, K. J., and Lee, S. J., "Studies on the Mold Filling in the Resin Transfer Molding Process: I. Numerical Simulation", Journal of the Korean Society for Composite Materials, Vol.11, 1998, p.8.

11. Adams, K. L. and Rebenfeld, L., "Permeability Characteristics of Multilayer Fiber Reinforcements. Part I: Experimental Observations", Polym. Compos., Vol.12, 1991, p.179.

12. Adams, K. L. and Rebenfeld, L., "Permeability Characteristics of Multilayer Fiber Reinforcements. Part II: Theoretical Model", Polym. Compos., Vol.12, 1991, p.186.

13. Wang, V. W., "Dynamic simulation with Graphics for the Injection Molding ofThree-Dimensional Thin Parts", Ph.D Thesis, Cornell

University, 1985.

14. Tadmor, Z., Broyer, E., and Gutfinger, C., "Flow Analysis Network(FAN) - AMethod for Solving Flow Problems in Polymer Processing", Polym. Eng. Sci., Vol.14, 1974, p.660.

15. Broyer, E., Gutfinger, C., and Tadmor, Z., "A Theoretical Model for the CavityFilling Process in Injection Molding", Trans. Soc. Rheol., Vol.19, 1975, p.423.